Transitions conserving parallel momentum in photoemission from the (111) face of copper

P. O. Gartland and B. J. Slagsvold
Department of Physics, The Norwegian Institute of Technology, 7034 Trondheim, Norway
(Received 22 July 1974; revised manuscript received 21 April 1975)

Photoelectric yields and directional photoemission spectra for clean (100) and (111) faces of copper measured with provision for varying the angle of incidence and the light polarization, and with photon energies up to 6.60 eV, are presented. Contrasting the structureless Fowler-like behavior of the (100) face, the (111) face shows two transitions conserving momentum parallel to the surface as peaks in the energy spectra and structure in the yield. A sharp peak excited by obliquely incident p-polarized light and responsible for a strong vector effect, is ascribed to a surface band in the band gap at the L point. This peak, located 0.40 ± 0.02 eV below the Fermi level in forward emission, disappears when the surface is significantly changed by oxygen exposure. At lower energies a wider peak identified with direct bulk transitions near the L point accounts for structure present in the yield even at normal incidence. From selection rules for momentum and energy, and parabolic approximations for the participating energy bands, theoretical predictions are derived for the peak positions at various frequencies and emission angles, and for the total yields. Parameters determined for the bulk transitions are in good over-all agreement with band-structure data, while an effective mass of $m_s^* = (0.42 \pm 0.05)m$, close to a corresponding mass in the bulk, is found for the surface band. The yields have thresholds exceeding the photoelectric work function, and their saturation beyond certain critical frequencies given by the band parameters, is reasonably well described by a matrix element pertinent to an image-potential surface barrier. For the surface band beyond its critical frequency the directional yield as well is in agreement with the theory. The emission is then confined to a forward cone becoming narrower with increasing photon energy.

I. INTRODUCTION

The task of completely specifying the process of photoemission from a solid in terms of the physical parameters is complicated by the uncertain role of the surface. While photoemission used to be viewed as a surface effect,[1] the importance of volume contributions[2] to the photocurrent was stressed by several authors.[3–5] Recent theories of photoemission[6,7] provide a basis for interpreting experiments that aim at a separation of the two contributions. However, in certain cases a metal surface may also possess intrinsic, localized quantum states,[8] and photoemission should, in fact, be a particularly suitable method for studying such states.[9]

Performing yield measurements, and applying the method of directional energy analysis,[10] we have studied the (111) face of a clean[11] copper crystal. Some comparative runs have also been made on the (100) face. Two peaks in our spectra are ascribed to transitions conserving momentum parallel to the surface. A similar observation of this conservation law has recently been reported for tungsten,[12] and for copper it is known that a large fraction of the electrons excited by direct $\vec{k}$-conserving transitions leaves a single crystal without scattering.[10] We invoke direct transitions across the band gap in a specific region of the Brillouin zone[13] to explain the wider, low-energy peak in our spectra. Like the spectrum of the (100) face of tungsten,[14] our (111) spectrum of copper shows a sharp peak just below the Fermi level. To our knowledge such a peak has not been seen in the photoemission spectra of copper before.[15] Postulating a band of surface states to exist within the s-p gap of copper, we are able to account for the behavior of the peak in great detail. There is no calculation of surface states within the s-p gap of copper that we know of, and the disagreement in the literature[9,16] regarding the existence of surface states in copper, appears to be concerned only with the d bands.

Our experimental system includes provision for varying the polarization and the angle of incidence of the light, as this is generally useful for surface studies. Evidence for the surface effect in aluminum was obtained in measurements where these parameters of the light were varied.[17] Now, the vector effect[18] is a well-known manifestation of the dependence of the photocurrent upon the polarization and the angle of incidence. For a clean macroscopically well-defined (111) face of copper we observed the effect as a strongly enhanced photocurrent due to the p-polarized component of the light upon going to large angles of incidence.[19] We attempted to describe the frequency dependence of the excess current by a formula for the classical surface effect. The fit was, however, inadequate in yielding a much too small value for the parameter representing the potential energy within the metal. Our observation of a surface peak in the energy distribution provides a more satisfactory interpretation of the strong vector effect in copper.

From a phenomenological model of the energy bands near the L point in copper, we derive in

Sec. II A a number of predictions for the behavior of the photoelectrons created in momentum-conserving transitions. In Sec. II B the same results are applied to the surface electrons by taking specific limits of certain band parameters. The application to our model states of a general formula for the directional yield is described in Sec. II C.

The details of the experimental technique and the results are given, respectively, in Secs. III and IV. Section V containing the discussion, is subdivided into separate parts on the bulk and surface transitions, respectively. The results of some supporting experiments may also be found here. Finally, in Sec. VI we summarize a number of conclusions.

II. THEORY

In this section we establish a theoretical framework needed to discuss two different contributions to the photocurrent from a copper crystal face which is parallel to the (111) planes of the lattice. We shall choose our coordinate system with its z axis along the direction of the surface normal, which also coincides with a ΓL direction in the Brillouin zone (BZ).

A. Bulk transitions

In doing photoelectron spectroscopy with an available maximum photon energy of 6.6 eV, we are limited to a rather narrow energy range of 2 eV for electrons emitted from clean faces of copper, which have work functions in excess of 4.5 eV.[11] Inspecting the band structure of copper[20] with this restriction in mind, we find that only the states associated with the band gap at the L point of the BZ boundary can contribute to our photocurrent by momentum-conserving transitions in the bulk. The structure of the energy bands in the vicinity of this gap is rather similar to that of the simplest kind of a nearly-free-electron gap. We approximate the bands by parabolic functions of the crystal momentum.[13] In doing this, we write for convenience constants α, β, a, and b instead of inverse effective masses, in the same way as we may substitute $\alpha_0 = \hbar^2/2m$ whenever the free-electron mass m occurs explicitly.

The initial states belong to the band which extends from the $L_{2'}$ state. Relative to the vacuum level the initial states have energies

$$E_i(\vec{\mathfrak{q}}, k_z) = -\Phi + E_{L_{2'}} - E_F + \beta q^2 - b(\tfrac{1}{2}G - k_z)^2 \,. \qquad (1)$$

$\vec{\mathfrak{q}}$, k_z are the components of the crystal momentum with $\vec{\mathfrak{q}}$ being parallel to the surface, Φ is the work function of the (111) face, and $E_F - E_{L_{2'}}$ is the depth of the $L_{2'}$ state below the Fermi level. $\frac{1}{2}\vec{G}$ is the crystal momentum of the L point.

Similarly, the final-state energies within the metal may be expressed as

$$E_f(\vec{Q}, K_z) = -\Phi + E_{L_1} - E_F + \alpha Q^2 + a(\tfrac{1}{2}G - K_z)^2 \,. \qquad (2)$$

The momentum components have now been designated by capital letters, and $E_{L_1} - E_F$ is the distance of the L_1 state above the Fermi level.

In vertical optical transitions, crystal momentum, as well as energy, is conserved. Thus $\vec{Q} = \vec{\mathfrak{q}}$, $K_z = k_z$, and $\hbar\omega = E_f - E_i$, but in order that excited electrons may appear as photoelectrons, their energy in the final state must be positive. This energy may also be expressed as $E_f = \alpha_0 p^2$ in terms of the momentum $\vec{p}(= -i\hbar\nabla)$ of the electrons outside the metal. For an ideal crystal surface parallel momentum must be conserved in the escape process. Thus $|\vec{Q}| = p_{\parallel} = p \sin w$ for electrons emitted in a direction making an angle w with the surface normal.

Combining the band relations (1) and (2) with the assumed conservation laws, we may write down the energy $E = E_f$ of a photoelectron in terms of the escape angle and the photon energy

$$E = \frac{a}{a+b}(\hbar\omega - \hbar\omega_c)\frac{\sin^2 w_c}{\sin^2 w_c - \sin^2 w} \,. \qquad (3)$$

Two new parameters, a critical photon energy $\hbar\omega_c$ and a critical angle w_c, have been introduced. They are given in terms of our basic model parameters by the relations

$$\begin{aligned} \hbar\omega_c &= E_{L_1} - E_{L_{2'}} + [(a+b)/a][\Phi - (E_{L_1} - E_F)] \,, \\ \sin^2 w_c &= \alpha_0(a+b)/(\alpha b + \beta a) \,. \end{aligned} \qquad (4)$$

The initial states must lie below the Fermi level in order to be occupied and contribute to photoemission at normal temperatures. Therefore, the maximum energy of the photoelectrons must be $E_{\max} = \hbar\omega - \Phi$. To establish a lower limit, we must specify $\hbar\omega$ relative to $\hbar\omega_c$. When $\hbar\omega < \hbar\omega_c$, all emission by the process being considered is confined to angles larger than w_c. The minimum value of momentum parallel to the surface is finite and corresponds to emission in the directions $w = 90°$. From Eq. (3) the minimum energy is then seen to be $E_{\min}(\hbar\omega) = [a/(a+b)](\hbar\omega_c - \hbar\omega)\tan^2 w_c$. Since this is finite, there must be a photoelectric threshold $\hbar\omega_t$ for this process, so that at the threshold $\hbar\omega_t = E_{\min}(\hbar\omega_t) + \Phi$. Solving for the threshold, we find

$$\hbar\omega_t = \frac{\Phi + [a/a+b)]\hbar\omega_c \tan^2 w_c}{1 + [a/(a+b)]\tan^2 w_c} \,. \qquad (5)$$

The minimum emission angle occurs when q increases to take the initial-state energy through the Fermi level. Substituting $E_{\max}$ in Eq. (3), we find a limiting angle w_l given by

$$\sin w_l = \sin w_c \left(1 + \frac{a}{a+b}\,\frac{\hbar\omega_c - \hbar\omega}{\hbar\omega - \Phi}\right)^{1/2} \,. \qquad (6)$$

When $\hbar\omega > \hbar\omega_c$, transitions for which $q = 0$ are allowed, and for increasing q the emission angle increases up to a limiting angle still given by Eq. (6), but now $w_l < w_c$. The minimum energy is then given by $E_{\min} = [a/(a+b)](\hbar\omega - \hbar\omega_c)$, and it will be observed in forward emission.

Finally, for the critical case $\hbar\omega = \hbar\omega_c$ photoelectrons with energies between 0 and $\hbar\omega - \Phi$ should emerge in the direction w_c.

B. Surface transitions

In free-electron-like metals the simplest band gaps are describable as a splitting of the free-electron states due to Bragg scattering by a single pseudopotential coefficient $V(\vec{G})$. However, there are solutions of the Schrödinger equation with energies within such a band gap.[8] When $V(\vec{G})$ is positive, it is possible to match some of these to exponentially decaying solutions of the Schrödinger equation outside the metal.[21] The resulting stationary states correspond to wave vectors with a complex component normal to the surface. In the presence of an imaginary component $i\kappa$ of the wave vector, the probability density of the states will have a factor $e^{2\kappa z}$ within the metal. Such states are therefore localized in the surface region, and they may be observable on a clean and crystallographically well-defined single-crystal face normal to the $\vec{G}$ which is responsible for the band gap.

The copper gap, while having a free-electron-like structure, is strongly influenced by the lower-lying d bands. Therefore, neither the simple criterion that $V(\vec{G})$ be positive in order that a surface state may exist, nor a more general criterion valid for narrow gaps[22] is strictly applicable. Nevertheless, we have checked the sign of $V(\vec{G})$. $V(\vec{G})$ is the product of an atomic form factor $v(G)$, which is positive for copper,[23] and the structure factor $S(\vec{G})$. For $\vec{G} = (2\pi/a)(1, 1, 1)$, when choosing the origin in an atomic site, we find $S = +1$. Thus, the sign of $V(\vec{G})$ is at least compatible with the existence of surface states in the band gap at the L point.

Since we claim that the transitions between the bulk states can be identified separately, additional states are needed to explain the observation of a sharp peak in our photoemission spectra. Lacking a theoretical prediction of such states, we postulate the existence of a set of surface states in the band gap at the L point of copper. We attempt to justify our postulate by making a detailed comparison between the theoretical predictions derived from it, and experimental observations.

For an ideal single-crystal face, crystal momentum parallel to the surface $\vec{q}$ is a good quantum number, and we assume that a (111) surface of copper has a band of energies given by

$$E_s(\vec{q}) = -\Phi - E_0 + \beta_s q^2 . \tag{7}$$

The bottom of the band is located a distance E_0 below the Fermi level, and the inverse mass parameter β_s may be different from the corresponding bulk quantity β.

With special choices for some parameters it is possible to use the results of Sec. II A to describe the narrow resonance observed in the angular photoemission spectra. The surface band replaces the band given by Eq. (1) as initial states. As final states we use the free-electron states in the vacuum for which $E_f = \alpha_0 p^2$. This corresponds to letting $b \to 0$, $\beta \to \beta_s$, and $E_F - E_{L_{2'}} \to E_0$ in all the results of Sec. II A. In particular, the expressions for the critical quantities of Eq. (4) become simply $\hbar\omega_{c,s} = \Phi + E_0$ and $\sin^2 w_{c,s} = \alpha_0/\beta_s = m_s^*/m$.

C. Photocurrent

To find the photocurrent per unit solid angle in a process where the momentum parallel to the surface is conserved, we use the expression[6]

$$\frac{dI}{d\Omega} = \frac{2em}{(2\pi)^2} \int \frac{d^3k_i}{(2\pi)^3} p\,|M(\vec{p}, k_i)|^2 . \tag{8}$$

The integral is taken over the initial states, and M is the matrix element of the perturbing Hamiltonian due to the lightfield. M is to be calculated between the initial states and a wave of unit amplitude impinging on the crystal from the outside, account being taken of the energy conservation.

For transitions in the bulk, we assume the squared matrix element to be basically of a form suggested by Mahan[6]

$$|M|^2 \propto \frac{1}{\omega^3} f(\theta, \hat{\epsilon})\,|T(p_z, K_z)|^2\,\delta(k_z - K_z)\,\delta(\vec{q} - \vec{Q}) . \tag{9}$$

With constant intensity of the incident light, the function f depends upon the angle of incidence θ and the polarization vector $\hat{\epsilon}$. The factor ω^3 is an explicit frequency dependence which results from the photon flux and a convenient transformation of the matrix element of the dipole operator. Additional frequency dependence due to that of the optical constants of copper has been neglected. T is the transmitted amplitude of the final state.

The integration of Eq. (8) can now be performed but, as repeatedly warned by Mahan, the integration is tricky because $\vec{Q}$, K_z depend upon $\vec{q}$, k_z through the energy conservation. We find

$$\frac{dI}{d\Omega} \propto \frac{f(\theta, \hat{\epsilon})}{\omega^3} \frac{(\hbar\omega - \hbar\omega_c)^{1/2} \sin^3 w_c}{(\sin^2 w_c - \sin^2 w)^{3/2}} |T(w)|^2 . \tag{10}$$

These electrons emerge in a definite direction relative to the surface normal with an energy given by Eq. (3). Since all momenta are now expressible in terms of w, T has been written as a function of a single argument. However, the explicit

form is needed to be able to proceed to find $I(\omega)$.

At low energies of the emitted electrons the step-potential-barrier model yields $|T|^2 \propto p_z^2$, but for the more realistic image-potential barrier, $|T|^2 \propto p_z$ should give a rather precise description.[24] In order to gain some insight into the pertinence of the specific choice for the surface-barrier model, the integration has been carried out for both models. The results are for the image- and step-potential barriers, respectively,

$$I_{\text{image}}(\omega) = \begin{cases} C_1[f(\theta,\hat{\epsilon})/\omega^3](\hbar\omega - \hbar\omega_t)/\cos^2 w_c\,, & \hbar\omega_c > \hbar\omega > \hbar\omega_t \quad (11a) \\ C_1[f(\theta,\hat{\epsilon})/\omega^3]/(\hbar\omega_c - \Phi)\,, & \hbar\omega > \hbar\omega_c\,, \quad (11b) \end{cases}$$

$$I_{\text{step}}(\omega) = \begin{cases} C_2[f(\theta,\hat{\epsilon})/\omega^3](\hbar\omega - \hbar\omega_t)^{3/2}\,, & \hbar\omega_c > \hbar\omega > \hbar\omega_t \quad (12a) \\ C_2[f(\theta,\hat{\epsilon})/\omega^3][(\hbar\omega - \hbar\omega_t)^{3/2} - (\hbar\omega - \hbar\omega_c)^{3/2}]\,, & \hbar\omega > \hbar\omega_c\,. \quad (12b) \end{cases}$$

C_1 and C_2 are constants of proportionality.

For transitions from the surface band we assume, in analogy to Eq. (9), the squared matrix element to be of the form

$$|M|^2 \propto [f_s(\theta,\hat{\epsilon})/\omega^3]|T|^2 \delta(\vec{q} - \vec{p}_{\parallel})\,,$$

where $\vec{p}_{\parallel}$ is the parallel momentum outside the metal. Also, Eq. (8) is now to be integrated over the two-dimensional initial momentum $\vec{q}$. Note that the optical factor $f_s(\theta,\hat{\epsilon})$ will be different from the previous one. If the surface states are not too sharply localized at the surface, it is perhaps reasonable to assume the same T as for the bulk transitions. Then all the results that we have obtained can be used for the surface transitions as well, when the appropriate limits of the parameters are taken.

III. EXPERIMENTAL

The measurements were carried out on a sample cleaned and maintained in a stainless-steel ultra-high-vacuum chamber with a base pressure below 10^{-10} Torr. The experimental setup inside the vacuum chamber is shown schematically in Fig. 1. Monochromatic light from a Hilger & Watts quartz prism monochromator with a xenon arc lamp could be focused on the specimen through one of two windows situated 90° apart on the cylindrical vacuum vessel. The maximum available photon energy was about 6.6 eV, as atmospheric absorption became prohibitive above this energy. The light could be made linearly polarized with sufficient intensity for frequencies up to 5.8 eV by inserting a polarizer in the light path.

The photoemission analyzer was constructed with the purpose of obtaining directional energy distribution curves (DEDC's), as well as energy distribution curves measured over a large acceptance angle (EDC's). In this work, however, only the more informative DEDC's will be presented. The analyzer consists of a system of two concentric hemispherical grids and a collector indicated in Fig. 1. Directional resolution was achieved by means of a channel electron multiplier behind a hole in the collector. Its total acceptance angle was about 6°, and the angle between the axis of the grid-collector system and the direction of the channel electron multiplier, was fixed to 25°. The analyzer was operated in the retarding field mode. The stopping potential V_R was applied to the second grid, while the first grid and the sample were grounded to provide a drift region free from disturbing electric fields. In directional measurements at low energies the elimination of disturbing electric and magnetic fields is found to be of extreme importance. Stray electric fields from charged insulators, windows, etc., inside the experimental chamber were eliminated by surrounding the sample by a copper cylinder attached to

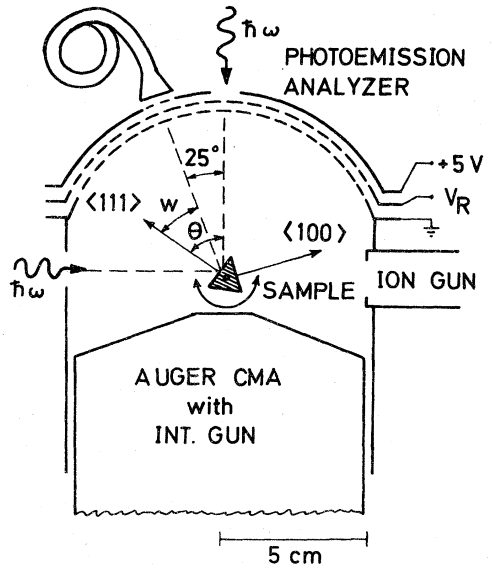

FIG. 1. Top view of the experimental setup inside the ultra-high-vacuum chamber.

the first grid as shown in Fig. 1. Ambient magnetic fields were reduced to below 50 mG by means of a pair of Helmholtz coils, and for electron energies $E \geq 0.3$ eV the maximum systematic error in w was estimated to be $\pm 3°$.

The spectra could be recorded in two different ways. At sufficiently high photocurrents the conventional ac-modulation technique[25] was applied using the channel electron multiplier as a current preamplifier. At low currents the ac technique gave too noisy signals, and the DEDC's were instead obtained by graphically differentiating the output from a counting rate meter. With a sufficiently low modulation amplitude ($V_{p-p} < 0.1$ V) the two methods gave identical results. However, nearly all the curves presented in this paper were obtained by the more convenient ac method.

When the crystal was rotated, DEDC's from each surface could be obtained at different polar angles of emission w. The azimuth angle was fixed, but the experiment was run with the crystal in two different mounting positions to permit measurements at two azimuth angles 180° apart. As is to be expected, the results showed no dependence upon this twofold rotation around the [111] axis. The polar angle w could not be changed independently of the angle of incidence of the light θ. However, using both entrance windows, while keeping w constant, we observed that the variation of θ caused changes only in the strengths of the structures, and not in their energy positions.

The measurements of the total yields were carried out as described previously.[19] However, the frequency dependence of the photon flux hitting the sample surface was investigated with improved reliability and accuracy over the whole range of frequencies. Thus, transmission losses in the optical windows were accurately corrected for, and freshly prepared sodium salicylate films of the recommended thickness were used.[26]

The sample was a single-crystal copper specimen with two faces of size 12×8 mm^2 cut and electropolished parallel to the (111) and (100) planes within 1°. It was suspended from a universal-motion crystal manipulator which permitted accurate adjustment of both the translational and the angular position. The cleaning of the crystal faces was accomplished by using the same cyclic treatment of ion bombardment and annealing as described earlier.[11] In the present experiment, however, the cleanliness of the surfaces was checked by Auger electron spectroscopy. The mounting positions of the cylindrical mirror, the Auger analyzer, and the combined ion gun and heat source are also shown in Fig. 1. The surfaces were considered to be clean when the Auger peaks from the major contaminants carbon, sulphur, and oxygen were reduced to the limit of detectability, which corresponded roughly to 5×10^{-3} times the height of the main copper peak $M_{2,3}VV$ at 60 eV.

IV. RESULTS

A. Directional energy distributions

Assuming that diffuse and inelastic scattering of electrons play a minor role at low photon energies, one expects DEDC's to carry information from regions of the Brillouin zone where the energy bands may be different. An anisotropy is, in fact, demonstrated for copper by the very different energy distributions obtained from the two surfaces. This is shown in Fig. 2 for the nearly forward direction and a photon energy of 6.4 eV. The emission from the (111) face is resolved into two peaks which are both absent from the (100) spectrum. Although the latter face might also deserve a detailed investigation, the results presented here are mainly from the (111) face. However, the DEDC's from the (100) face are most suitable for estimating the energy resolution. From the steep slope of the Fermi edge in the sharpest spectra recorded, the experimental broadening was found to be maximum 0.10 eV for electron energies up to 2.0 eV.

DEDC's from the (111) face are shown in Fig. 3 for different photon energies. A low-energy peak labeled 1 appears for photon energies above 5.8 eV. With increasing photon energy it grows continuously and moves to lower energies. Another structure, the strong peak labeled 2, is present even for $\hbar\omega = 5.40$ eV and is stationary in initial energy at 0.4 eV below the Fermi level. The

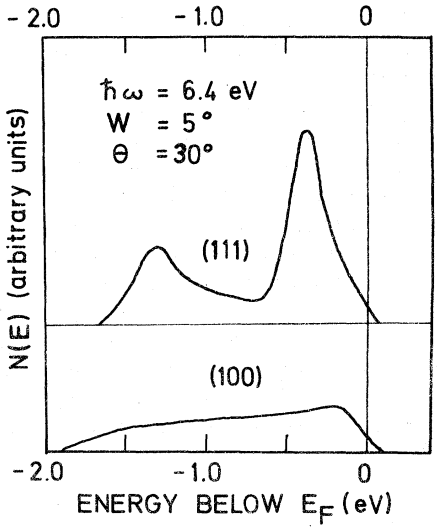

FIG. 2. Experimental energy distribution curves for nearly forward emission ($w = 5°$) from Cu(111) and Cu(100). The photon energy is 6.40 eV, and the vertical scale is the same for both surfaces.

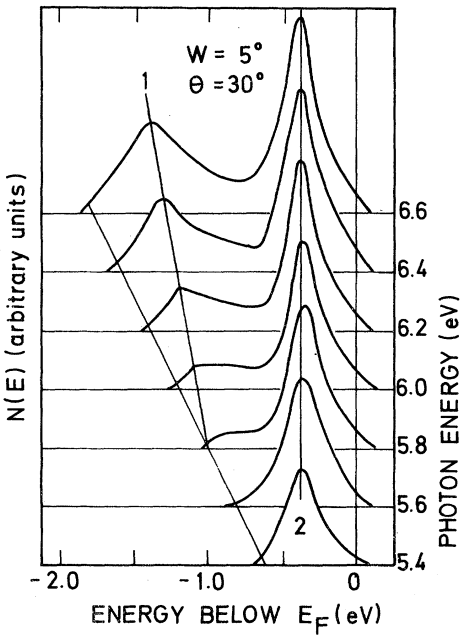

FIG. 3. Experimental energy distribution curves for nearly forward emission ($w = 5°$) from Cu(111) and photon energies between 5.4 and 6.6 eV.

curves in this figure, as well as those in Fig. 2, have been normalized to have an area proportional to the directional yield at each frequency.

For $\hbar\omega = 6.60$ eV, where both peaks are strongly developed, DEDC's for different polar angles w are presented in Fig. 4. The curves are here normalized to have an area in proportion to the directional yields measured for the different crystal orientations corresponding to the given values of w. The variation in the excitation conditions caused by the simultaneous change in θ, could not be corrected for in a simple manner. This arises because the low-energy peak was much less sensitive to changes in the angle of incidence than peak 2. We observe from Fig. 4 that both structures move to higher energies with increasing w. At a certain emission angle the strong peak goes through the Fermi level, and the peak height is dramatically reduced. The weaker structure 1 seems to follow a similar path at a slower rate, but at higher angles it is recognized more like a shoulder than a peak. At angles larger than $w = 50°$, the distributions are characterized by a triangular shape changing very little with increasing angle up to $w = 70°$.

B. Excitation conditions

Using linearly polarized light we have found that peak 2 is excited only when the light has an electric field component normal to the surface. This structure in our spectra must be responsible for the strong vectorial photoeffect that we observed in yield measurements on the (111) face.[19]

Because the polarizer became strongly absorbing above 5.8 eV, it could not be used to investigate the polarization dependence of structure 1. However, using both entrance windows at a constant emission angle, we observed structure 1 to have a much weaker θ dependence than the high-energy peak. Since the latter is the only structure present for $\hbar\omega = 5.15$ eV, its θ dependence is represented by the total yield as shown in Fig. 1 of Ref. 19. In accordance with its polarization dependence, peak 2 is hardly observable with light of normal incidence, while the low-energy peak is still present.

C. Yield measurements

In a total yield measurement the various contributions to the current superimpose to make the interpretation of any observed structure quite difficult. From the measured DEDC's of the (111) face we are able to distinguish between three contributions of different behavior. In the first place, there is a sharp peak in the DEDC which dominates the total yield at high angles of incidence. Second, there is a weaker structure which is also present at $\theta = 0°$, where the sharp peak is almost totally suppressed; and third, there is a structureless background. The total yield measured at $\theta = 70°$, and shown in Fig. 5, is therefore taken as repre-

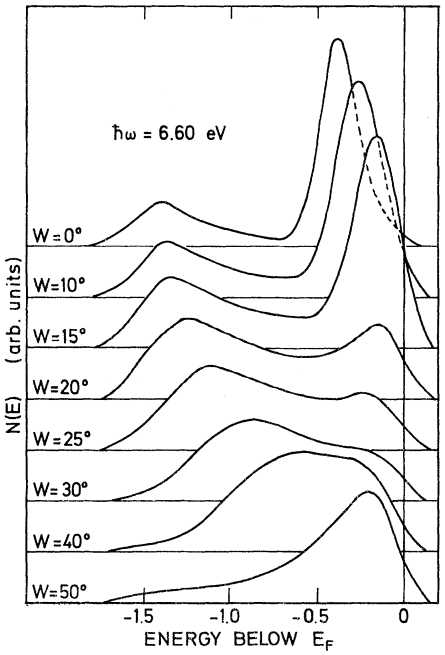

FIG. 4. Experimental energy distribution curves of photoelectrons emitted at various angles w relative to the surface normal of the (111) face of copper. The photon energy is 6.60 eV.

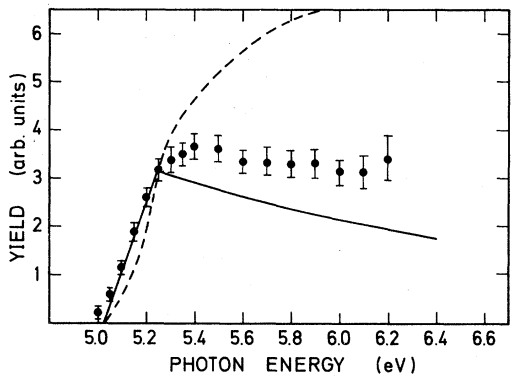

FIG. 5. Total photoelectric yield from the surface transition of the (111) face of Cu. Experimental points (full circles), representing the total yield as measured for $\theta = 70°$, are compared to the theoretical yields calculated with a step-potential barrier (dashed line), and an image-potential barrier (solid line). Both theoretical curves are scaled to the experimental value at $\hbar\omega = 5.25$ eV.

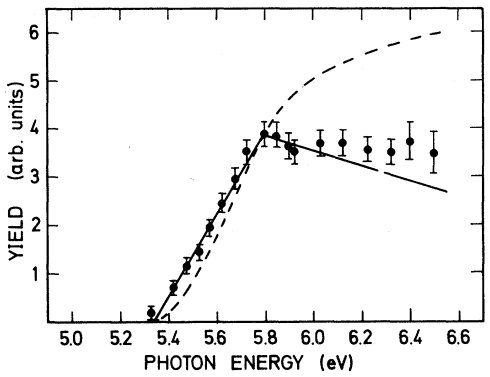

FIG. 7. Total photoelectric yield through a (111) surface from bulk direct transitions across the s-p band gap at the L point of Cu. Experimental values (full circles), representing the yield in excess of the Fowler line in Fig. 6, are compared to theoretical curves calculated with a step-potential barrier (dashed line), and an image-potential barrier (solid line). Both theoretical curves are scaled to the experimental value at $\hbar\omega = 5.80$ eV.

sentative of the frequency dependence of the yield from the strong peak alone. This curve is nearly the same as the one presented in Fig. 2 of Ref. 19, except that the light intensity this time has been controlled to a greater accuracy at high frequencies. The improved accuracy also revealed some characteristic features in the normal incidence yield from the (111) face. This can most clearly be seen in Fig. 6, where the square root of the yield has been plotted for both the (100) and (111) faces. While the results for the (100) face fit a straight line very well over the entire frequency range, the measurements for the (111) face show a more complicated dependence upon the frequency. In order to determine the photoelectric work function Φ, a straight line was fitted to

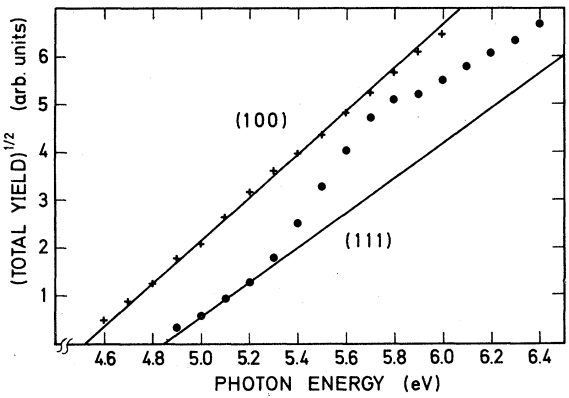

FIG. 6. Square root of the normal incidence yields from the (111) and (100) faces of Cu, showing the deviation from a straight Fowler line for the (111) face above $\hbar\omega \simeq 5.3$ eV.

the low-frequency data as usual. From the intercept of this line with the axis, we get $\Phi(111) = 4.85$ eV, which is slightly lower than previously measured.[11] At a photon energy of about 5.3 eV, the experimental values start to increase more rapidly than predicted by the simple Fowler theory, indicating a new kind of threshold. We now assume that the extrapolation of the Fowler line above 5.3 eV represents the background, or a structureless part of the emission, similar to the DEDC's for the (100) face. We may subtract this contribution from the total yield and retain only the part of the DEDC's characteristic of structure 1. Figure 7, showing this net yield, should be compared with Fig. 5. The peaks 1 and 2, although of a very different nature, have yield curves of quite similar shapes, as characterized by a threshold $\hbar\omega_t$ and an abrupt change of slope at a certain photon energy $\hbar\omega_c$. Since most of the interesting information is contained in these characteristic photon energies, no absolute calibration of the yield curves has been carried out.

The yield was also measured as a function of the emission angle w, but here only the contribution from the dominating peak could be easily separated. Using the curve in Fig. 1 of Ref. 19 to correct for the variation due to a changing angle of incidence, the area under the peak was taken as representative of the yield. The result is shown in Fig. 8 for two different frequencies. The intensity increases with the emission angle w up to a certain angle w_t, where it suddenly drops. Thus, the current is concentrated in cones around the surface normal, the cone angle becoming smaller with increasing photon energy.

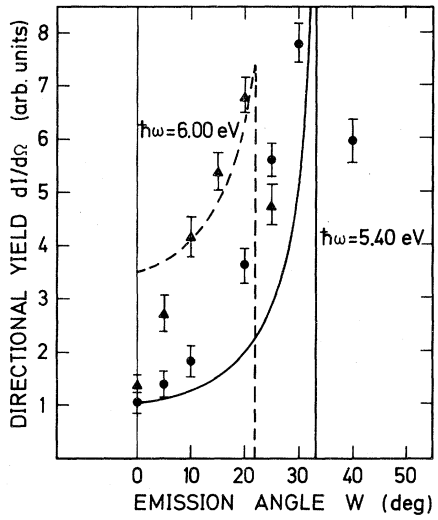

FIG. 8. Directional yields from the surface transitions at the (111) face of Cu. Experimental values obtained for $\hbar\omega = 5.40$ eV (full circles) and $\hbar\omega = 6.00$ eV (full triangles) are compared with theoretical curves (solid line, dashed line) without broadening. The theoretical amplitude is adjusted to fit one single point ($w = 0°$, $\hbar\omega = 5.40$ eV).

V. DISCUSSION

A. Bulk transitions

In their pioneering work on photoemission from cesiated copper, Berglund and Spicer[4] identified a structure in their EDC's from a polycrystalline film due to direct, $\vec{k}$-conserving transitions around the L-symmetry point in the BZ. Later work[13] has confirmed this identification, and accurate measurements on the boxlike structure appearing in the EDC's from cesiated films have been analyzed to give a detailed description of the band structure in the vicinity of the s-p band gap. This is in good agreement with the band-structure calculations of Burdick.[20]

Assuming specular reflection at the surface ($\vec{q}$ conserved) in the directional energy analysis on the low-index surface (111) of a Cu single crystal, we expect the boxlike structure in EDC's to be resolved into a peak whose position depends upon the photon energy and the polar angle of emission w, as described by Eq. (3). As seen from Figs. 3 and 4 the low-energy structure has both frequency and angular dependences characteristic of the direct transitions for $\hbar\omega > \hbar\omega_c$. Data allowing a quantitative description of this contribution to the photocurrent can be obtained from Fig. 7. Independent of any specific choice of the barrier transmission function, the characteristic frequencies of the theoretical model are determined to be $\hbar\omega_t = 5.35 \pm 0.05$ eV and $\hbar\omega_c = 5.80 \pm 0.05$ eV. The remaining two parameters in Eq. (3) were determined by fitting the equation to a total of 16 measured peak positions taken from curves similar to those of Fig. 4. In a least-squares fit the parameters were found to be $a/(a+b) = 0.53$ and $w_c = 56°$. With these parameter values the final energy given by Eq. (3) is as shown in Fig. 9. The experimental results in the pertinent range of frequencies have also been plotted. From this figure we see that the direct transition peak should appear at angles larger than w_c for $5.35 < \hbar\omega < 5.8$ eV. At these photon energies, however, the DEDC's are rather narrow, and no unambiguous identification could be achieved.

TABLE I. Characteristic frequencies $\hbar\omega_t$ and $\hbar\omega_c$, the critical angle w_c, and the band parameter $a/(a+b)$ of the photoelectrons created in direct transitions near the L point of Cu(111).

	$\hbar\omega_t$(eV)	$\hbar\omega_c$(eV)	w_c	$\frac{a}{a+b}$
This work	5.35 ± 0.05	5.80 ± 0.05	$56° \pm 5°$	0.53 ± 0.10
Band structure[a]	5.27	5.93	44.5°	0.66
Previous work[b]	5.40	6.13	48.5°	0.60

[a]Calculated with data from Ref. 20.
[b]Calculated with parameters of Ref. 13.

In Table I we have made a comparison between our values for the parameters $\hbar\omega_c$, $\hbar\omega_t$, $a/(a+b)$, and w_c, and those obtained from Eqs. (4) and (5) using known experimental[13] and theoretical[20] data for the band parameters. Possible systematic errors of the order of ± 0.05 eV in the determina-

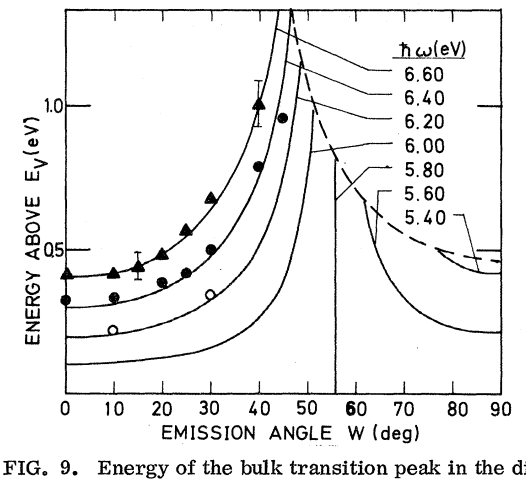

FIG. 9. Energy of the bulk transition peak in the directional spectrum from the (111) face of Cu as a function of the emission angle. Theoretical curves (solid lines) shown for the pertinent range of photon energies were obtained from Eq. (3) by a least-squares fit to the measured peak positions with $\hbar\omega = 6.20$ eV (open circles), $\hbar\omega = 6.40$ eV (full circles), and $\hbar\omega = 6.60$ eV (full triangles). Dashed curve shows the maximum electron energy $\hbar\omega - \Phi$.

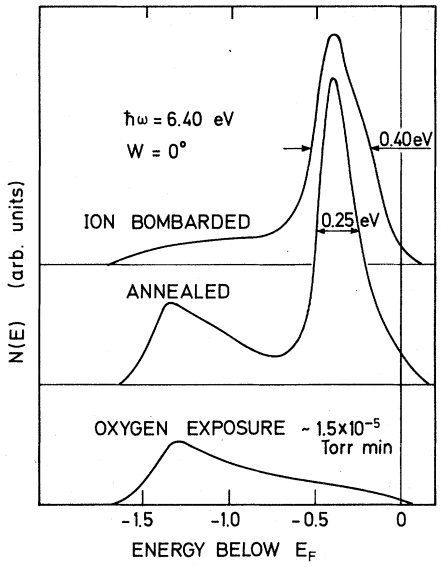

FIG. 10 Experimental energy distribution curves for normal emission ($w = 0°$) from the (111) face of Cu, as obtained after various surface treatments. Photon energy is 6.40 eV.

tion of the peak positions, would give rather large uncertainties on our values for $a/(a+b)$ and w_c. The data tabulated for this work are obtained entirely from our own experiments, and in view of the very different ways the reference data have been obtained, we find the over-all agreement quite satisfactory. This confirms the interpretation that a considerable part of the photoelectrons due to direct transitions around the L-symmetry point leaves the crystal unscattered.[10] A similar observation has been reported on single-crystal films of silver.[27] However, when the surface is subject to ion bombardment, the number of lattice imperfections increases to a depth[28] comparable to the escape depth of the photoelectrons.[29] The quasielastic scattering is then considerably enhanced, and any directional information tends to vanish. This is borne out in the observed disappearance of the low-energy peak upon ion bombardment as shown in Fig. 10.

In Fig. 10 we also see that oxygen adsorption dramatically reduces the strength of the high-energy peak, while structure 1 is left rather unchanged. This clearly demonstrates that the low-energy peak cannot be due to electrons transferred from the high-energy peak by inelastic collisions. At photon energies larger than used here, inelastically scattered electrons always pile up at the low end of the EDC's,[30] but for $\hbar\omega < 6.6$ eV the corresponding contribution to the photocurrent should be negligible.

One should expect[6] the direct transition to have a polarization dependence $(\vec{G}_{111} \cdot \hat{\epsilon})^2$. Our observation disagrees with this expectation. At normal incidence, with $\hat{\epsilon}$ perpendicular to $\vec{G}_{111}$, we do see the structure in the DEDC's, and the characteristic shape of the yield curve can hardly be explained in another way. However, copper is not a free-electron metal, and it may be necessary to modify the theory that we are using. In a recent theoretical paper[31] the strict polarization dependence is greatly relaxed in silver by going beyond the 2-OPW (orthogonalized plane wave) theory. The calculations show that a polarization normal to the appropriate $\vec{G}$ may cause a non-negligible contribution to the transition probability of direct transitions from energy levels in the vicinity of the Fermi level. Since copper and silver are closely related metals, the lack of a simple $(\vec{G}_{111} \cdot \hat{\epsilon})^2$ dependence upon polarization gets some theoretical justification from the calculations of Schaich.

In theoretical works on photoemission, model calculations are commonly performed using a simple step potential for the surface barrier. A more realistic model would use an image-potential barrier. The two surface-barrier models give quite different shapes of the yield curves, as shown in Fig. 7. At the critical frequency $\hbar\omega_c$, the image-potential-barrier model shows a discontinuous change of slope, while the yield curve with a step-potential barrier only changes from positive to negative curvature at $\hbar\omega_c$. The theoretical curves scaled to the experimental yield at $\hbar\omega_c$ show clearly that only the image-potential barrier gives a fair fit. One might object that the subtraction of the background in the experimental yield curve is somewhat artificial, and systematic errors are probably present in the curve in Fig. 7. Nevertheless, the abrupt change of slope at $\hbar\omega_c$ is clearly visible even in the total yield in Fig. 6. Thus the insufficiency of a step-potential model is experimentally demonstrated.

In conclusion, we find that a contribution to our photocurrent can be rather consistently ascribed to momentum-conserving bulk transitions near the L point in the band structure of copper.

B. Surface emission

Having concluded that the bulk effects associated with the $L_1 - L_{2'}$ gap of copper have been separately accounted for, we observe that the width of the peak 2 in Fig. 3 is significantly smaller than usually found in bulk spectra. Our proposal is that the peak is caused by transitions from quantum states localized in the surface region of clean, well ordered (111) faces of copper.

Emission by the surface effect has a $(\hat{z} \cdot \hat{\epsilon})^2$ dependence upon polarization,[6] but since the surface normal is a symmetry axis in the problem, the same dependence may also be expected for other

kinds of a surface emission. Combined with the effect of the optical discontinuity, such a polarization dependence results in a characteristic variation in the yield with the angle of incidence—a vector effect.[19] Furthermore, a surface emission is expected to be sensitive to the conditions at the surface, i.e., to the amount of contamination and disorder. Figure 10 shows the surface peak to be sensitive to oxygen exposure, but a rather large amount of oxygen was needed to suppress the peak completely. However, it has been found in low-energy-electron-diffraction (LEED) experiments that the (111) surface of copper is far more resistant to oxygen contamination than the (100) face,[32] and no significant changes in the LEED pattern from Cu(111) are observed until the exposure reaches the 10^{-5} Torr min region. Thus, the photoemission peak disappears at about the exposure necessary to change the (111) face significantly.

Disordering, such as may arise upon ion bombardment, should also affect surface states. Now it appears from Fig. 10 that the surface peak is hardly affected at all by the bombardment damage. The only visible change is that the energy width at half-maximum has increased from 0.25 eV for the well-annealed surface to 0.4 eV for the bombarded face. This indicates that some of the directional information has been lost as a result of an increased diffuse refraction, just as for the peak due to bulk transitions. But, whereas the latter can spread over the entire spectrum, the surface peak is still confined to within the upper 0.4 eV.

The survival of the surface peak in the presence of bombardment damage may seem strange. However, as discussed in a previous paper,[11] there are indications that even during rather heavy bombardment, the copper surface retains a certain short-range order. This statement is supported by the failure to completely destroy the LEED pattern from copper.[33]

Since the localization of the peak 0.4 eV below the Fermi level in forward emission is independent of the photon energy, it is clearly an initial-state effect. Assuming a value of 0.75 eV for $E_F - E_{L_{2'}}$,[13] the bottom of the surface band is localized 0.35 eV into the band gap above the $L_{2'}$ state of the bulk. Since this energy separation is small compared to that of other bands, notably the d bands, it may be used to estimate the localization in space from $\vec{k}\cdot\vec{p}$ perturbation theory at the $L_{2'}$ point.[34] For small real $\frac{1}{2}\vec{G}-\vec{k}$ in the ΓL direction we have $E - E_{L_{2'}} = -\hbar^2(\frac{1}{2}G - k)^2/2m^*_{i\parallel}$. Applying this formula in the case of a small imaginary $\frac{1}{2}G - k = i\kappa$, and taking[20] $m^*_{i\parallel} \approx 0.32m$, we calculate the attenuation length of the probability density to be $\frac{1}{2}\kappa = 3$ Å, which is close to the minimum value of 2.2 Å as calculated from Jones's result $\kappa_{\max} = 2mV_G/\hbar^2 G$ for the nearly-free-electron model.[35] Such a small length would mean that most of the probability density is localized to within the outmost layer of unit cells. However, our mental picture of surface states resulting from a simple matching procedure is then hardly adequate, and our estimate must be considered as qualitative.

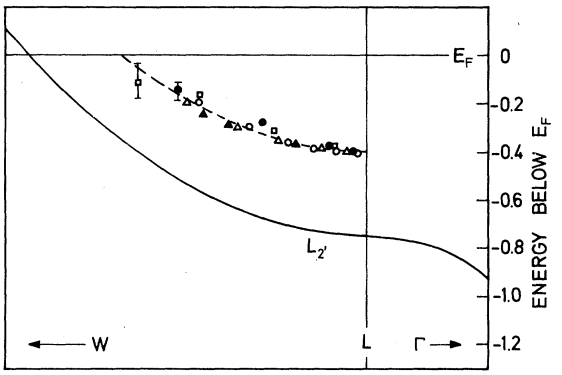

FIG. 11. $L_{2'}$ bulk band in the vicinity of the L point, and the occupied part of the surface band of the (111) face of Cu. Experimental data from Ref. 13 have been used to draw the $L_{2'}$ band. The surface band (dashed line) was obtained from a least-squares fit to the measured peak positions at different photon energies $\hbar\omega = 5.40$ eV (open circles), 5.60 eV (open triangles), 6.00 eV (full triangles), 6.40 eV (open squares), and 6.60 eV (full circles).

To test the predictions derived from our theoretical assumptions, the peak position was measured as a function of the emission angle w in steps of 5° for five different photon energies. The results were fitted to the surface band of Eq. (7). This is shown in Fig. 11 where the observed peak positions (E, $\sin w$, $\hbar\omega$) have been converted into initial-state parameters (E_i, q). The dashed line represents a least-squares fit to the data points. Allowing for additional systematic uncertainties in reading angles and energies, the fitted surface effective mass and energy are $m^*_s = (0.42 \pm 0.05)m$ and $E_0 = 0.40 \pm 0.02$ eV. From these numbers we calculate a critical angle of $w_{c,s} = 40° \pm 3°$, a threshold of $\hbar\omega_{t,s} = 5.02 \pm 0.03$ eV, and a critical photon energy of $\hbar\omega_{c,s} = 5.25 \pm 0.03$ eV.

For comparison, several numerical values are available for the effective mass describing the curvature of the $L_{2'}$ band normal to the ΓL direction. The numbers $m^*_{i\perp} = 0.46m$, $0.37m$, and $0.34m$ were obtained from cyclotron resonance,[36] photoemission measurements,[13] and band-structure data,[20] respectively. If we think in terms of $\vec{k}\cdot\vec{p}$ perturbation theory, then $m^*_{i\perp}$ is mainly determined by coupling to the d bands, which are at least 1.75 eV lower in energy. It is perhaps not too unreasonable to expect the surface band to have a similar coupling, and the small difference of 0.35 eV in energy separation would then result

in m_s^* being about $0.04m$ larger than $m_{i\perp}^*$. With the uncertainties present we cannot make a conclusive statement concerning the difference $m_s^* - m_{i\perp}^*$, but m_s^* does seem to characterize a true copper property.

In the same way as for the bulk transitions, we may compare the measured yields to the calculated ones to investigate the barrier models. Since the surface states seem to be so highly localized, it is not obvious that the same T should apply for both bulk and surface transitions. The comparison between measured and calculated yields made in Fig. 5 again shows the image potential to give the closest approximation, although the change of slope at $\hbar\omega_{c,s}$ is not as sharp as it was at $\hbar\omega_c$. Also, the rather well defined threshold at $\hbar\omega_{t,s} = 5.00 \pm 0.05$ eV agrees well with that calculated from the angular measurements.

Since one has to correct for the change in the angle of incidence, the directional yields could be measured with less accuracy than the total ones. In Fig. 8 angular yield curves obtained from the data are compared with the predictions from Eq. (10). The error bars on the experimental points include only reading errors, but we note that at low emission angles the experimental yield deviates from the theoretical. This may be a real effect, or simply a systematic error connected with the use of very-large angles of incidence to obtain forward emission. Irrespective of the presence of small systematic errors, the qualitative agreement is, however, encouraging.

The phenomenological model of a surface band characterized by the two parameters m_s^* and E_0 gives a detailed and good description of the sharp surface peak in our spectra, and we conclude that such a surface band is an intrinsic property of the (111) face of pure copper.

VI. CONCLUSIONS

The number of photoelectrons excited from Cu(111) by monochromatic light of photon energies up to 6.6 eV, were measured with respect to the dependence on the final electron energy, the direction of emission, and on the energy, the polarization, and the direction of the incoming photons. Two well-separated structures in the energy distribution curves for various angles of emission were observed. A wide peak in the low-energy part of the spectra was ascribed to direct transitions across the s-p band gap of copper, while a sharper peak just below the Fermi energy was explained by postulating the existence of a surface band within the bandgap. The assignment of a peak in the spectra to surface transitions was based on the sharpness of the peak, its unique polarization dependence, and its sensitivity to oxygen contamination. Assuming the surface band to have a parabolic dependence of energy on the wave vector parallel to the surface, a surface effective mass of $m_s^* = (0.42 \pm 0.05)m$, close to the transverse mass of the bulk, was found. The energy minimum was located 0.40 ± 0.02 eV below the Fermi level.

The frequency dependences of the directional and total yields were compared to calculations based on simple parabolic expressions for the bulk and surface band valid in a limited region of the momentum space. Two characteristic photon energies entering the equations were identified experimentally for both the surface and volume transitions. Owing to the conservation of the parallel momentum, the thresholds $\hbar\omega_{t,s} = 5.00 \pm 0.05$ eV and $\hbar\omega_t = 5.35 \pm 0.05$ eV exceeded the photoelectric threshold Φ. At the corresponding critical frequencies $\hbar\omega_{c,s} = 5.25 \pm 0.05$ eV and $\hbar\omega_c = 5.80 \pm 0.05$ eV the yield curves changed markedly. The shapes of the measured yields could only be reasonably well explained within the model when an approximation pertinent to an image-potential barrier was used for the transmission coefficient.

In agreement with the predictions of the model, the electrons emitted by surface transitions emerged within a cone centered on the surface normal, the cone angle becoming narrower with increasing photon energy.

ACKNOWLEDGMENTS

We wish to express our gratitude to Dr. E. Østgaard and Dr. R. O. Jones for reading and commenting helpfully on drafts of this paper, and to the Norwegian Research Council (NAVF) for financial support.

[1] I. Tamm and S. Schubin, Z. Phys. 68, 97 (1931).
[2] H. J. Fan, Phys. Rev. 68, 43 (1945).
[3] A. Meessen, J. Phys. Radium 22, 308 (1961).
[4] C. N. Berglund and W. E. Spicer, Phys. Rev. 136, A1030 (1964).
[5] F. Wooten and T. Huen, J. Opt. Soc. Am. 57, 102 (1967).
[6] G. D. Mahan, Phys. Rev. B 2, 4334 (1970).
[7] W. L. Schaich and N. W. Ashcroft, Phys. Rev. B 3, 2452 (1971).
[8] V. Heine, Proc. Phys. Soc. Lond. 81, 300 (1963).
[9] F. Forstmann and J. B. Pendry, Z. Phys. 235, 75 (1970).
[10] U. Gerhardt and E. Dietz, Phys. Rev. Lett. 26, 1477 (1971).
[11] P. O. Gartland, S. Berge, and B. J. Slagsvold, Phys. Norv. 7, 39 (1973).
[12] R. R. Turtle and T. A. Callcott, Phys. Rev. Lett. 34, 86 (1975).
[13] I. Lindau and L. Wallden, Phys. Scr. 3, 77 (1971).
[14] B. Feuerbacher and B. Fitton, Phys. Rev. Lett. 30, 923 (1973).
[15] A preliminary report on this peak was presented at the NORDITA Solid Surfaces Conference, Copenhagen, Nov.

1974 (unpublished).
[16]R. V. Kasowski, Phys. Rev. Lett. 33, 83 (1974).
[17]S. A. Flodström and J. G. Endriz, Phys. Rev. Lett. 31, 893 (1973).
[18]D. W. Juenker, J. P. Waldron, and R. J. Jaccodine, J. Opt. Soc. Am. 54, 216 (1964).
[19]P. O. Gartland, S. Berge, and B. J. Slagsvold, Phys. Rev. Lett. 30, 916 (1973).
[20]G. A. Burdick, Phys. Rev. 129, 138 (1963).
[21]F. Forstmann, Z. Phys. 235, 69 (1970).
[22]J. B. Pendry and S. J. Gurman, Surf. Sci. 49, 87 (1975).
[23]M. L. Cohen and V. Heine, in *Solid State Physics*, edited by H. Ehrenreich, F. Seitz, and D. Turnbull (Academic, New York, 1970), Vol. 24, p. 200.
[24]L. A. MacColl, Phys. Rev. 56, 699 (1939).
[25]W. E. Spicer and C. N. Berglund, Rev. Sci. Instrum. 35, 1665 (1964).
[26]R. Allison, J. Burns, and A. J. Tuzzolino, J. Opt. Soc. Am. 54, 747 (1964).
[27]T. Gustafsson, P. O. Nilsson, and L. Walldén, Phys. Lett. 37, A121 (1971).
[28]J. A. Venables, in *Atomic Collision Phenomena in Solids*, edited by D. W. Palmer, M. W. Thompson, and P. W. Townsend (North-Holland, Amsterdam, 1970), p. 132.
[29]C. R. Brundle, J. Vac. Sci. Technol. 11, 212 (1974).
[30]P. O. Nilsson and I. Lindau, in *Band Structure Spectroscopy of Metals and Metal Alloys*, edited by D. J. Fabian and L. M. Watson (Academic, London, 1973), p. 55.
[31]W. L. Schaich, Phys. Status Solidi 66, 527 (1974).
[32]I. Marklund, S. Andersson, and J. Martinson, Ark. Fys. 37, 127 (1968).
[33]S. Andersson (private communication).
[34]W. A. Harrison, *Solid State Theory* (McGraw-Hill, New York, 1970), p. 173.
[35]R. O. Jones, in *Surface Physics of Semiconductors and Phosphors*, edited by C. A. Scott and C. E. Reed (Academic, New York, 1975).
[36]J. F. Koch, R. A. Stradling, and A. F. Kip, Phys. Rev. 133, A240 (1964).